

Gottesman-Kitaev-Preskill state preparation by photon catalysis

Miller Eaton,^{*} Rajveer Nehra, and Olivier Pfister

Department of Physics, University of Virginia, 382 McCormick Rd, Charlottesville, VA 22904-4714, USA

Continuous-variable quantum-computing (CVQC), the most scalable implementation of QC to date, requires non-Gaussian resources for reaching exponential speedup and performing quantum error correction, using error encoding states such as the Gottesman-Kitaev-Preskill (GKP) states. However, GKP state generation is still an experimental challenge. We show theoretically that photon catalysis, the interference of coherent states with single-photon states followed by photon-number-resolved detection, is a powerful enabler for quantum state engineering, in particular the preparation of exact displaced single-photon states, of squeezed cat states, and of GKP states.

INTRODUCTION

Quantum Computing (QC) offers the possibility to solve certain computational problems which are intractable in the realm of classical computation [1, 2]. In the last couple of decades, QC has been widely explored over discrete variables, mostly qubits, and several architectures have been proposed and experimentally realized [3]. Another flavor, equally universal, of QC makes use of continuous variables (CV) [4–6], such as the position and momentum of a quantum harmonic oscillator or, analogously, the amplitude- and phase-quadrature amplitudes of the quantized electromagnetic field. The interest of CVQC comes primarily from the large-scale, and highly scalable, implementations that have been experimentally demonstrated of measurement-based QC substrates such as cluster entangled states with at least 60 simultaneously entangled qumodes [7] and one million sequentially entangled qumodes, accessible two at a time [8]. A fault tolerance threshold has been proven to exist for CVQC [9] for the Gottesman-Kitaev-Preskill (GKP) quantum error correction protocol [10, 11]. This protocol uses error code states which have a non-Gaussian Wigner function, a required resource in CV quantum information for CVQC exponential speedup [12], for entanglement distillation [13] and Bell inequality violation [14], and for quantum error correction [15].

The experimental generation of non-Gaussian states is therefore a key effort in quantum information science. Single-photon states have been generated and characterized using heralding detection of downconverted photon pairs [16–19]. More sophisticated techniques, such as photon subtraction and addition [20], have been very promising advances due to their feasibility. In photon subtraction, Fig.1(a), a nonclassical state of light impinges onto a highly unbalanced, say transmissive, beam-splitter and a photon-number-resolving (PNR) detector, ideally, or at least a single-photon sensitive one, detects the reflected light. Conditioned on the detection of n photons, one can show that the transmitted light is, to a reasonably good approximation, the state $a^n |\psi\rangle$, where ψ denotes the initial state of light and a the photon an-

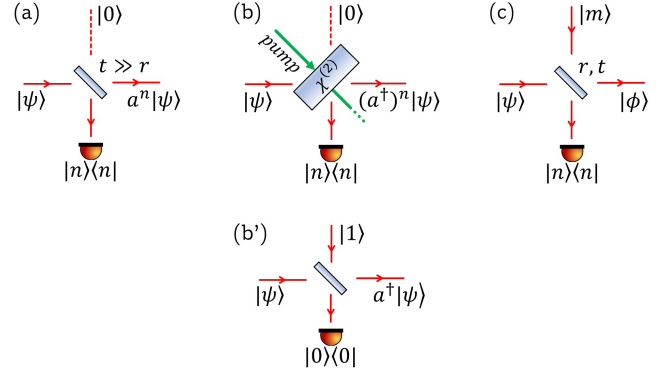


FIG. 1. Various feasible techniques for generating quantum states with non-Gaussian Wigner functions. Diagram (a) depicts n photon subtraction, (b) and (b') denote variants of n and single-photon additions, respectively, and (c) generalizes the previous cases for an m fock state with arbitrary beamsplitter parameters and n photon detection.

ihilation operator [21, 22]. This was recently generalized to multimode light [23]. Photon subtraction cannot work on coherent states, of course, but photon addition, Fig.1(b), does [24] [Figure 1(b') displays a variant]. In Fig.1(c), a more general process is presented, called photon catalysis [25], which is reviewed and developed in Ref. 26. This technique is derived from the quantum scissors scheme [27] and consists in interfering a quantum state (not necessarily pure) with a Fock state and performing PNR detection of one beamsplitter output. The beamsplitter is no longer necessarily unbalanced and its coefficients are parameters of the process as well. Note that PNR is now an experimentally available resource thanks to superconducting transition-edge sensors [19, 28, 29].

In this paper, we explore the use of photon catalysis to generate non-Gaussian states of interest to CVQC, in particular exact displaced single-photon states, Schrödinger cat states, and GKP states. No squeezed states are required, the needed resources being coherent states and linear optics, single-photon states, and PNR detection.

PHOTON CATALYSIS

In the rest of this paper, we take the restriction of photon catalysis in Fig.1(c) to $m=1$, i.e., to single-photon input

$$|\text{out}\rangle_{ab} = \sum_{m=0}^{\infty} \psi_m \sum_{k=0}^m \binom{m}{k}^{\frac{1}{2}} r^{m-k} t^k \left[t\sqrt{m-k+1} |m-k+1\rangle_a |k\rangle_b - r\sqrt{k+1} |m-k\rangle_a |k+1\rangle_b \right], \quad (1)$$

where ψ_m are the Fock amplitudes of the input $|\psi\rangle_a$, $r, t \in \mathbb{R}$, and $r^2 + t^2 = 1$. If, say, output a is sent to a PNR detector which measures n photons, then output b is projected into the state

$$|\phi\rangle_b \propto \sum_{\ell=0}^{\infty} \psi_{\ell+n-1} \binom{\ell+n-1}{\ell}^{\frac{1}{2}} t^{\ell} (nt^2 - \ell r^2) |\ell\rangle_b. \quad (2)$$

If the beamsplitter is designed so that destructive quantum interference $nt^2 = \ell r^2$ occurs, then the corresponding Fock state $|nt^2/r^2\rangle$ is absent from the output. Note that the state amplitudes are shifted by $n-1$ in the process. When postselecting on $n=1$, this shift disappears and, by setting $r^2 = 1/(q+1)$ for the beamsplitter, one can remove the q -photon amplitude:

$$|\phi_q\rangle_b = \sum_{\ell=0}^{\infty} \psi_{\ell} \left(\frac{q}{q+1} \right)^{\frac{\ell}{2}} \left(1 - \frac{\ell}{q} \right) |\ell\rangle_b. \quad (3)$$

If $|\psi\rangle$ has a maximum number ℓ_{\max} of amplitudes and if $q \gg \ell_{\max}$, then the Fock-state filtering is almost perfect: only ψ_q is removed and the other amplitudes are practically unchanged.

However, the number of free parameters allows us to Fock-filter a state in several different ways. Rather than postselecting $n=1$ and tuning the beamsplitter, it would be much more advantageous, from an experimental point of view, to postselect as little as possible and use PNR detection to the fullest. Let us also fix $r = t = \frac{1}{\sqrt{2}}$, then

$$|\phi\rangle_b \propto \sum_{\ell=0}^{\infty} \psi_{\ell+n-1} \binom{\ell+n-1}{\ell}^{\frac{1}{2}} 2^{-\frac{\ell}{2}} (n-\ell) |\ell\rangle_b, \quad (4)$$

thereby removing the n -photon Fock state from the b output if n photons are detected in port a . Again, one should keep in mind that the state amplitudes ψ_k are shifted by $n-1$ in the process, hence this operation of photon catalysis is more complex than just Fock-state filtering. However, as we now show, photon catalysis can nontrivially generate *exact* displaced single-photon states, as well as arbitrarily good approximations of non-Gaussian states

resource states, but we keep the option of $n > 1$ in PNR detection. For an input mode $|\psi\rangle_a |1\rangle_b$, ψ being an arbitrary state, the output state is [30, 31]

that are of interest in quantum information processing, such as Schrödinger-cat states and GKP quantum error code resource states. In all the rest of the paper, we will consider either a coherent-state input, $|\psi\rangle = |\alpha\rangle$, or inputs derived from previous photon catalysis steps, $|\psi'\rangle = |\phi\rangle$.

Numerical modeling

To practically apply photon catalysis to arbitrary quantum states, we developed a numerical procedure to take an input density matrix, possibly an impure quantum state, and transform it to a new state following photon catalysis. We begin by defining a generic beamsplitter operation, projector, and input density matrices as

$$U_{ab} = e^{\theta(ab^\dagger - a^\dagger b)} \quad (5)$$

$$P_n = (|n\rangle\langle n|)_a \otimes \mathbb{1}_b \quad (6)$$

$$\rho_a^{\text{in}} = (|\psi\rangle\langle\psi|)_a \quad (7)$$

$$\rho_b^{\text{in}} = (|1\rangle\langle 1|)_b \quad (8)$$

where $r = \cos\theta$ is the reflection coefficient. After the beamsplitter, but before the detection event, the new density matrix is

$$\rho_{ab} = U_{ab} \rho_a^{\text{in}} \otimes \rho_b^{\text{in}} U_{ab}^\dagger. \quad (9)$$

We then apply the projective measurement of mode a by an ideal detector and normalize to obtain the resulting density matrix of mode b , given by

$$\rho^{\text{out}} = \frac{\text{Tr}_a[\rho_{ab} P_n]}{\text{Tr}[\rho_{ab} P_n]}. \quad (10)$$

Imperfect detection can be modeled by including a loss beamsplitter followed by a perfect detector as depicted in Fig.2, where we trace out over the lost mode. In this case we now have a vacuum input mode to consider, so a new input state of $\rho_c^{\text{in}} = (|0\rangle\langle 0|)_c$, a loss beamsplitter $U_{ac} = e^{\xi(ac^\dagger - a^\dagger c)}$ where $\eta = \cos\xi$ is the detector efficiency, and a modified projector, $P_n^\eta = (|n\rangle\langle n|)_a \otimes \mathbb{1}_b \otimes \mathbb{1}_c$. Eq. (9)

becomes

$$\rho_{abc} = U_{ac}\rho_{ab} \otimes \rho_c^{in} U_{ac}^\dagger. \quad (11)$$

As before, we apply the projective measurement of the detector, but must now also trace out over the lost beam-splitter port in addition to the detected mode. Our final state is now

$$\rho^{out,\eta} = \frac{Tr_{ac}[\rho_{abc} P_n^\eta]}{Tr[\rho_{abc} P_n^\eta]}. \quad (12)$$

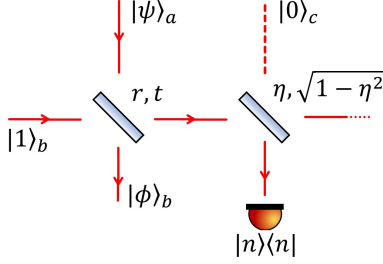


FIG. 2. Loss model. Photon catalysis with an imperfect detector can be modeled by placing a beamsplitter of reflectivity η with vacuum input before an ideal detector, where the other output is lost via a partial trace.

In subsequent sections of this work, we explore the possibility to perform cascaded photon catalysis, by which we use the output of one procedure as the input to a second process. When performing the cascaded photon catalysis, the first iteration begins with a coherent state input, so $|\psi\rangle_a = |\alpha\rangle$ for the first time through. To perform subsequent photon catalysis steps, the density matrix from Eq. (10) can be fed back as the the input for Eq. (7) to repeat the process as many times as desired, where θ and n can be chosen independently. Finally, we can compute the fidelity between a target state, ρ^T , and the result of our process, ρ^{out} , which we define by

$$F = \left| Tr \left[\sqrt{\sqrt{\rho^{out}} \rho^T \sqrt{\rho^{out}}} \right] \right| \quad (13)$$

When performing cascaded photon catalysis calculations, we only consider the case where $\eta = 1$, as the tensor product between the input state and vacuum state Hilbert spaces causes an exponential increase in computational expense with each additional vacuum mode added. For all of our numerical simulations, we limited the Hilbert space dimension to 40.

EXACT DISPLACED SINGLE-PHOTON STATES

The use of optical displacements is very important for implementing a variety of operations in continuous-variable

quantum information, since the Weyl-Heisenberg group of field quadrature shifts is the CV analog of the Pauli group for qubits [4, 12, 32, 33]. These displacements can be experimentally realized by combining the state to be displaced with a coherent state at a highly unbalanced beamsplitter [34] — with, say, high reflection for the state to be displaced and low transmission for the coherent state impinging on the other port. However, this method does require a partial trace over the other output port, yielding a statistical mixture that only approaches the exact displaced state as the reflectivity approaches unity, which in turn limits the amount of displacement. By contrast, photon catalysis is not subject to this limitation and can generate an exact displaced single-photon state.

Lossless case

We start with an input coherent state $|\psi\rangle = |\alpha\rangle$. Denoting the beamsplitter operator by $U_{ab} = \exp[\theta(ab^\dagger - a^\dagger b)]$ (where $r = \cos \theta$ is the reflection coefficient), we get

$$|out\rangle_{ab} = U_{ab} D_a(\alpha) |0\rangle_a b^\dagger |0\rangle_b \quad (14)$$

$$= (ta^\dagger - rb^\dagger) |r\alpha\rangle_a |t\alpha\rangle_b. \quad (15)$$

Conditioning on the detection of n photons in output a , i.e., we get

$$|\phi\rangle_b \propto {}_a\langle n | out \rangle_{ab} \quad (16)$$

$$\propto (nt - \alpha r^2 b^\dagger) |t\alpha\rangle_b. \quad (17)$$

We can then evaluate the overlap of $|\phi\rangle_b$ with a single-photon state displaced by β :

$$\langle 1 | D^\dagger(\beta) | \phi \rangle \propto nt(t\alpha - \beta) - \alpha r^2 [1 + \beta^*(t\alpha - \beta)]. \quad (18)$$

Normalizing Eq. (17) and taking $\alpha, \beta \in \mathbb{R}$ yields the fidelity

$$F = e^{-|\beta - t\alpha|^2} \frac{|nt(\beta - t\alpha) + r^2\alpha(1 + t\alpha\beta - |\beta|^2)|^2}{r^4|\alpha|^2 + t^2(n - r^2|\alpha|^2)^2}. \quad (19)$$

Examining this result, we see that, if $r^2|\alpha|^2$ is specifically chosen to be an integer so that $n = r^2|\alpha|^2$ photons are detected, then $F = 1$ for $\beta = \sqrt{|\alpha|^2 - n} = \alpha t$. This is the same as the limit case given by Ref. 34 where $\alpha \rightarrow \infty$ while $t \rightarrow 0$ and we replace the detector with a partial trace. However, here, the beamsplitter retains $t > 0$, the limit case not being needed to reach exact displacement. Therefore, we see that by tuning the reflectivity of a beamsplitter and post-selecting on the desired n detection, it is possible to use photon catalysis with a coherent state to prepare an exact displaced single-photon state of displacement amplitude $\beta = t\alpha$.

Lossy case

If we now consider an imperfect detector of quantum efficiency $\eta < 1$, the final state given by Eq. (12) is no longer pure and the fidelity with the target displaced Fock-state is no longer unity.

However, the fidelity can be improved slightly by modifying the displacement of the target state, $\rho^T = D(\beta)|1\rangle\langle 1|D(\beta)^\dagger$. In this case, we postulate, and numerically verify, that the maximum fidelity is achieved when

$$\alpha = \frac{\sqrt{n}r}{\eta} \quad (20)$$

$$\beta = \frac{1}{\eta}\sqrt{\alpha^2 - n} \quad (21)$$

and this value approaches unity as $t \rightarrow 0$ as illustrated in Fig. 3C, where the Wigner functions for various parameters are evaluated numerically using the open-source python codes QuTip [35] and Strawberry Fields [36]. In order to verify that the codes perform as expected, we computed the above photon catalysis step using QuTip and confirmed that the output state is identically a displaced Fock state for correctly chosen parameters. The Wigner functions displayed in Fig. 3 are plotted for three different values of initial coherent state amplitude and demonstrate that the output state slowly approaches the displaced Fock state as α is tuned, with and without losses.

SCHRÖDINGER CAT STATES

We now turn to Schrödinger-cat coherent superpositions (SCSs), which are of the type

$$|SCS_\pm(\beta)\rangle = N(|\beta\rangle \pm |-\beta\rangle), \quad (22)$$

where N is a constant. These non-Gaussian states have been proposed for quantum computing [37] and small-amplitude optical SCSs have been created by several methods [22, 38–41] but there has yet to be a reliable approach to generate larger photon-number SCSs. Methods have been proposed to “breed” SCSs using two smaller SCSs, a beamsplitter, and conditional detection to create a larger SCS of amplitude $\sqrt{2}\beta$ [42, 43] but these approaches become unrealistic for scaling due to a low success probability and a large prerequisite number of initial small SCSs.

Most SCS preparation methods result in a squeezed cat state, $S(r)|SCS_\pm(\beta)\rangle$, where $S(r) = \exp[r(a^{\dagger 2} - a^2)/2]$ is the single-mode squeezing operator. To our knowledge, the largest created optical SCS to-date made use of two

squeezed vacuum resources and a breeding step to create a squeezed SCS with $\beta = 2.15$ and a fidelity of 0.86 [44].

Using photon catalysis without any initially squeezed resource and only three detection steps, we show that one can create a state that approaches an exact squeezed SCS of amplitude $\beta = \sqrt{5}$, -4.34 dB of squeezing, and a calculated fidelity of $F \geq 0.99$. The general idea is somewhat counterintuitive: consider, for example, the “odd” SCS,

$$|SCS_-(\beta)\rangle = \frac{1}{\sqrt{\sinh|\beta|^2}} \sum_{n=0}^{\infty} \frac{\beta^{2n+1}}{\sqrt{(2n+1)!}} |2n+1\rangle, \quad (23)$$

which only contains odd photon numbers. Naïvely, it would be tempting to consider using photon catalysis to filter the even Fock components from a coherent state in an attempt to approximate an odd SCS. However, this approach would require cascaded stages which would “undo” one another in general because of the shift of the probability amplitudes by $n - 1$, at each stage, when $n > 1$. Thus, the previously filtered Fock amplitudes in a cascaded scheme do reappear, in general, after the next stage. Nonetheless, and remarkably, cascaded photon catalysis *can* be used to generate excellent approximations to *squeezed* SCSs — which are useful to generate the GKP resource states crucial to CV quantum error correction, as we will see in the next section.

Experimental protocol

We turn to the protocol, which is cascaded photon catalysis with $n = 5, 3, 1$, Fig. 4, on an input coherent state, here of amplitude $\alpha = \sqrt{14}$, with the first two steps following Eq. (4) and the last one Eq. (2) (unbalanced beamsplitter).

The effect of the first step on the state amplitudes is displayed in the top panel of Fig. 5, while the bottom panel shows a comparison of the resulting state, after displacing back to the origin, with an SCS and a squeezed SCS. Serendipitously, it appears that the result is close to a squeezed SCS.

The first projective PNR measurement acts to eliminate the $|5\rangle$ component from the initial coherent state, while the second and third photon catalysis steps effectively act to shift and rescale the remaining Fock-component coefficients. This results in a highly accurate approximation of a displaced, squeezed, odd-photon number SCS. When comparing the result of the cascaded photon catalysis with a target state given by

$$\rho^T = D(\delta)S(r)|SCS_-(\beta)\rangle\langle SCS_-(\beta)|S(r)^\dagger D(\delta)^\dagger, \quad (24)$$

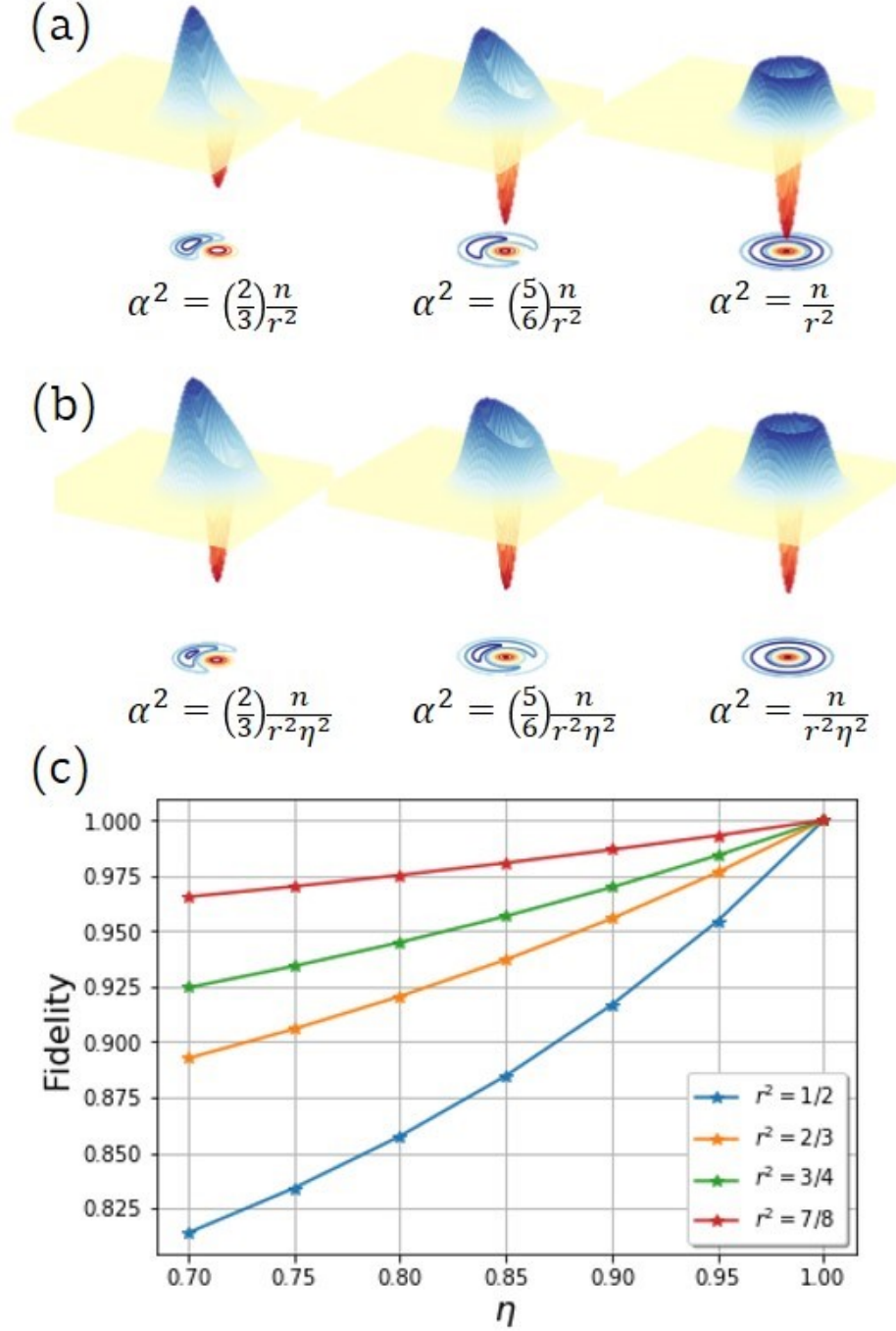


FIG. 3. (a): Wigner functions for lossless photon catalysis per Eq. (17). As the amplitude of the initial coherent state approaches the optimal ratio, the output Wigner function becomes that of a displaced single-photon Fock State. When $\alpha^2 = \frac{n}{r^2}$, the fidelity between the two states is unity. (b): Wigner functions for photon catalysis with detector efficiency $\eta = 0.9$. (Amplitudes have the same ratio of optimal values as in (a)) (c): Maximum fidelity achievable with a displaced Fock-state of displacement $\beta = \frac{1}{\eta}\sqrt{\alpha^2 - n}$ for detector efficiency η when the beamsplitter parameter r is varied.

our results show near perfect fidelity with an odd SCS of amplitude $\beta = \sqrt{5}$ and -4.34dB squeezing ($F = 0.993$), but also good agreement with larger SCSs of different squeezing, such as $\beta = \sqrt{10}$ [$\sqrt{16}$] squeezed at -7.24dB [-9.21dB] where the fidelity is 0.95 [0.90]. After apply-

ing a displacement operation ($D(-1.086)$) to bring the output state back to the origin, the Wigner function is plotted in Fig. 6.

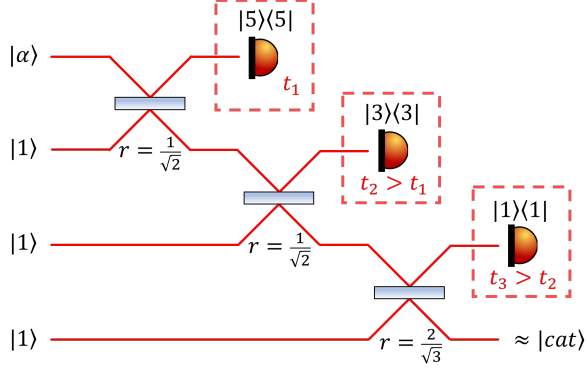


FIG. 4. Protocol for generating the approximate SCS using photon catalysis. The initial coherent state has amplitude $\alpha = \sqrt{14}$, and is successively interfered with single-photon Fock states on two balanced beamsplitters followed by a third beamsplitter with $r = \frac{2}{\sqrt{3}}$. Detection events occur successively, at times $t_1 < t_2 < t_3$, and are photon-number resolved to be $n = 5, 3$, and 1 respectively.

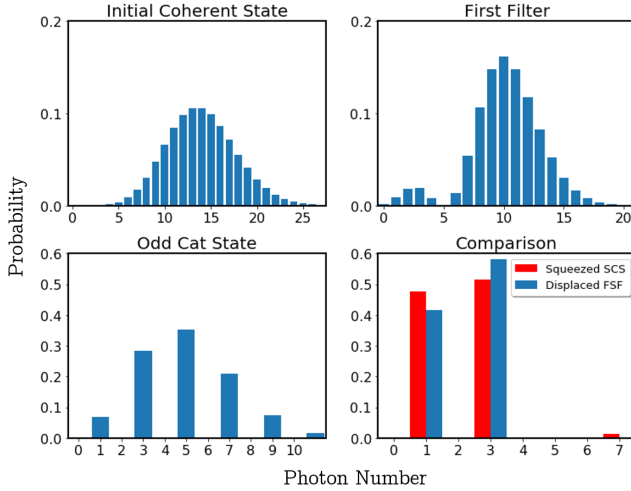


FIG. 5. Photon number probability amplitudes for various states. Top: distributions for coherent state input and the quantum state after the first detection step. Bottom: distributions for an odd photon-number SCS and for a squeezed SCS (red) compared to the displaced result from cascaded photon catalysis (blue).

GOTTESMAN-KITAEV-PRESKILL STATES

One of the practical uses of SCSs is the ability to approximate the Gottesman-Kitaev-Preskill (GKP) state [10], whose use has shown to yield a fault tolerance threshold for CVQC [9].

GKP state from SCS states

Here, we adapt an experimental proposal of Vasconcelos et al. [45] to our cascaded photon catalysis method of producing SCSs in order to create a hexagonal-lattice GKP, or “hex GKP,” state. The essence of their original idea is depicted in Fig. 7.

By entangling two squeezed SCS on a balanced beam-splitter and performing a homodyne measurement of $p = 0$ on one output, the output of the other port is projected into a state exhibiting a series of evenly spaced Gaussian peaks along the x quadrature axis where the peak amplitudes follow a binomial distribution about a central peak at $x = 0$, and the peak width is determined by the SCS squeezing. Repeating an identical protocol with two of these outputs serves to increase the number of peaks by elevating the order of the binomial distribution. After many iterations and in the limit of large initial squeezing, this method accurately approximates an ideal GKP state.

Hexagonal lattice GKP state

One principle advantage exhibited by the GKP encoding scheme is an inherent resistance to shift errors in the conjugate position and moment quadratures x and p . However, the recently formulated hex GKP state given by Ref. 46 improves upon the initial square lattice state by being able to correct larger displacement errors. As a hexagonal lattice in phase space, the hex GKP state can now account for shift errors with a new upper-bound phase space radius of $r \leq \sqrt{\frac{\pi}{3d}}$, as opposed to $r \leq \sqrt{\frac{\pi}{2d}}$ intrinsic to the original, where d is the dimensionality of the code space. This hex GKP state can be explicitly written as

$$|\mu_{\text{hex}}\rangle \propto \sum_{n_1, n_2 = -\infty}^{\infty} e^{-\frac{i}{2}(\hat{q} + \sqrt{3}\hat{p})\sqrt{\frac{4\pi}{d\sqrt{3}}}(dn_1 + \mu)} e^{i\hat{q}\sqrt{\frac{4\pi}{d\sqrt{3}}}n_2} |0\rangle, \quad (25)$$

where $\mu = 0, \dots, d-1$ labels the specific GKP state in the code space. To make the state physically realizable in the case of finite energy, the state can be modulated by a Gaussian envelope of width Δ [46]. The finite energy hex GKP state is thus given by

$$|\mu_{\text{hex}}^{\Delta}\rangle \propto e^{-\Delta^2 \hat{n}} |\mu_{\text{hex}}\rangle \quad (26)$$

where \hat{n} is the number operator, $a^{\dagger}a$. Taking inspiration from [45], we imagine applying the protocol from Fig. 7 to identical outputs of our photon catalysis process in the hopes to approximate a hex GKP state. However,

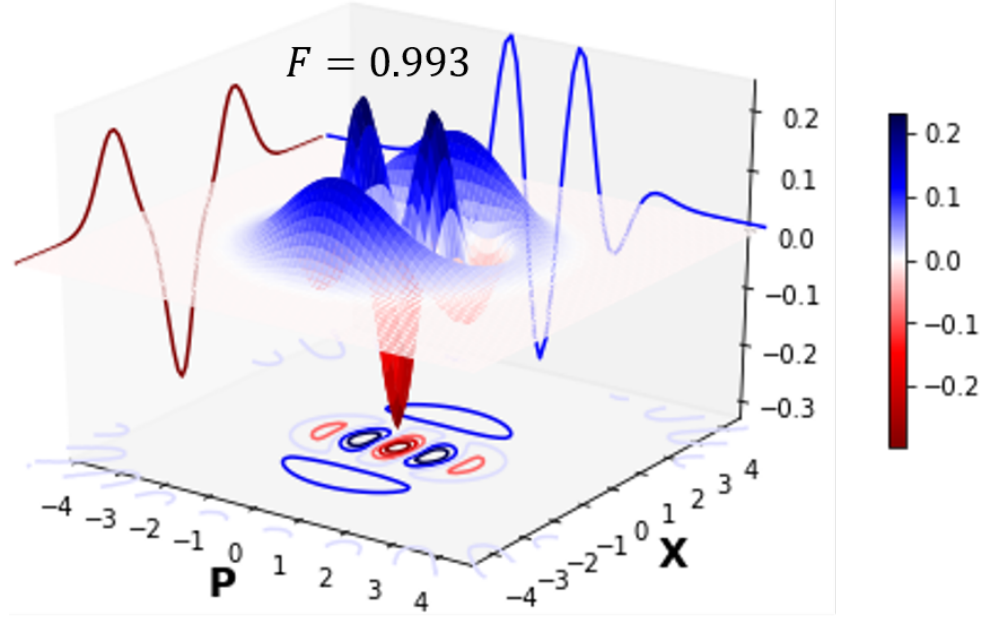


FIG. 6. Wigner function for the triply photon catalyzed coherent state. $F \geq 0.99$ [$F \geq 0.95$] with the ideal squeezed SCS state of amplitude $\beta = \sqrt{5}$ [$\beta = \sqrt{10}$] and squeezing of -4.34dB [-9.21dB].

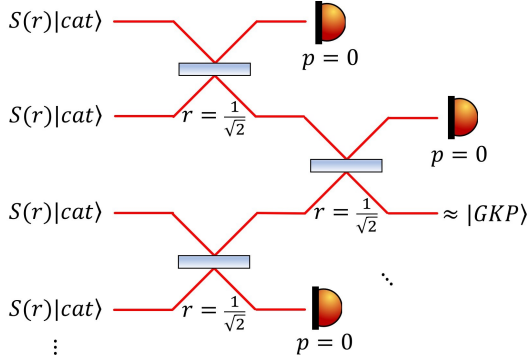


FIG. 7. Protocol developed in Ref. 45 where the first two iterations are shown. Interfered squeezed SCSs conditioned by $p = 0$ homodyne detection approximates a GKP state; repeating the process with previous outputs increases accuracy.

instead of beginning with squeezed SCSs, we directly use the outputs from the cascaded photon catalysis processes we described, which are in fact approximate squeezed SCSs with an additional displacement. As our results will demonstrate, the necessary displacement operations we would need to apply at each input to have the prerequisite squeezed SCSs for the protocol depicted in Fig. 7 can be commuted to a single displacement following the protocol. Now, instead of working in the photon number basis, we work in the p -quadrature basis and define the projector $P_0 = (|p = 0\rangle\langle p = 0|)_a \otimes \mathbb{1}_b$ for the homodyne measurement. Taking the outputs of our cascaded photon catalysis, we perform the calculations

$$\rho_{ab} = U_{ab}\rho_a^{\text{out}} \otimes \rho_b^{\text{out}}U_{ab}^\dagger \quad (27)$$

$$\rho^{\text{final}} = \frac{\text{Tr}_a[\rho_{ab}P_0]}{\text{Tr}[\rho_{ab}P_0]} \quad (28)$$

$$\rho^T = ND(\delta) |\mu_{\text{hex}}^\Delta\rangle \langle \mu_{\text{hex}}^\Delta| D(\delta)^\dagger \quad (29)$$

where U_{ab} is a balanced beamsplitter and N is a normalization factor for our new target state when calculating the fidelity. Remarkably, after a single iteration of this process (requiring only two initial inputs) the final state is very near a finite energy hex GKP state up to a displacement that came from our inputs being displaced SCSs. After displacing back to the origin, the final state approximates $|\mu_{\text{hex}}^\Delta = 3\rangle$ of code dimension $d = 6$, where the modulating Gaussian envelope has phase-space width $\Delta = 0.644$. We plot the Wigner function and photon probability distribution of the final result, which are displayed in Fig. 8, where the calculated fidelity with the ideal finite-energy hex GKP state is $F = 0.997$.

CONCLUSION

In this work, we have further explored the photon catalysis process [25] where interfering a single-photon with an input state on a beamsplitter can result in specifically engineered non-Gaussian quantum states contingent upon beamsplitter parameters and conditioned by PNR detection. By using a coherent state as an input, we

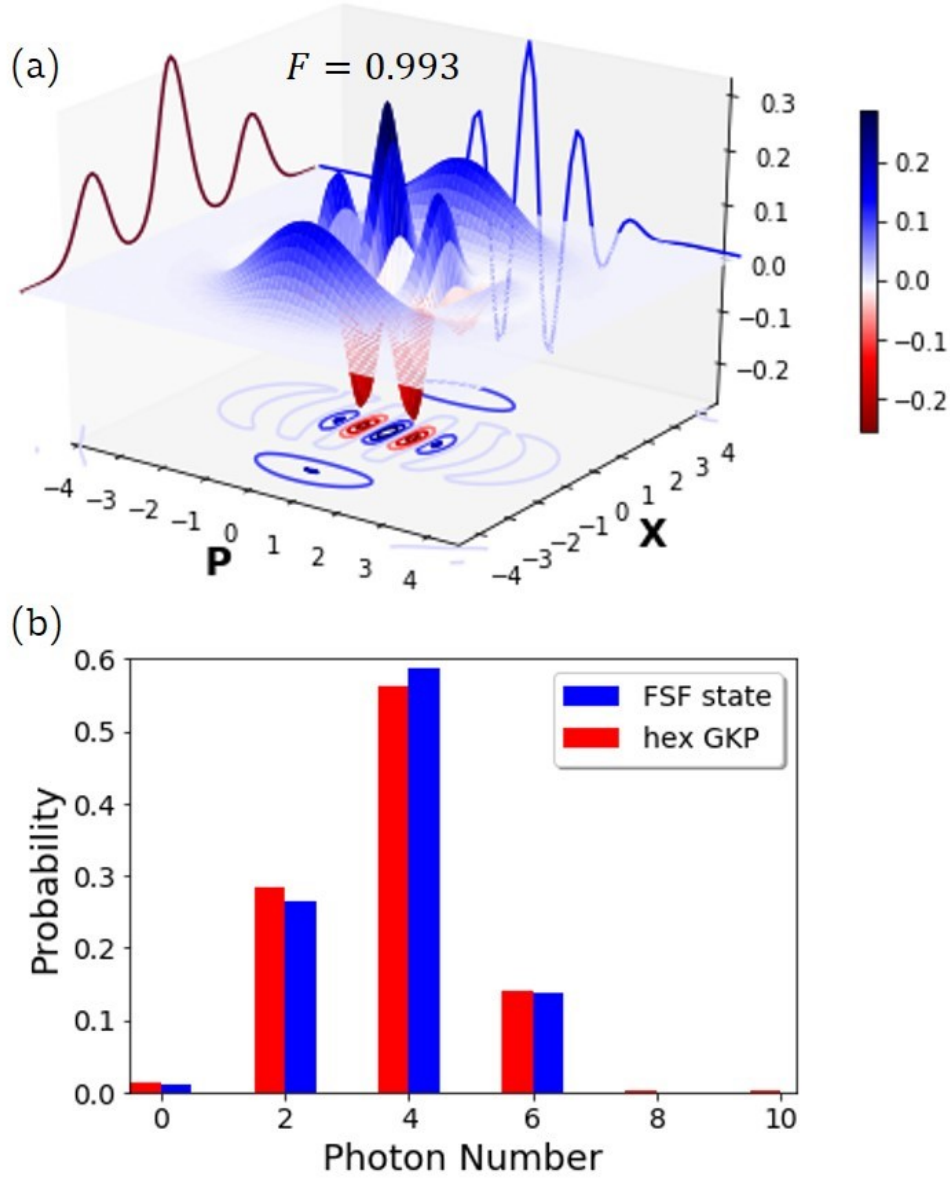


FIG. 8. (a): Approximate Hex GKP state $|\mu_{hex} = 3\rangle$ of code dim 6 where finite energy peaks are modulated by a Gaussian of width $\Delta = 0.644$. (b): Photon number distributions for the approximate state from iterative photon catalysis (blue) and ideal finite-energy state (red), where the fidelity is 0.997.

demonstrated that one photon catalysis step can implement arbitrary displacements on the single photon Fock state and preserve state purity. Further, by cascading the photon catalysis process, we are able to filter out multiple photon number components and accurately approximate relatively large superpositions of coherent states, which to our knowledge is the largest proposed optical

SCS without breeding or the need for large-number Fock states. From here, we show that it is possible to enact the method from [45] and generate hex GKP states contingent upon successful homodyne detection. One particular point of note is that while the cascaded photon catalysis produces a displaced, squeezed SCS, this displacement can be commuted with the beamsplitter and homo-

dyne detection operations allowing for a single required displacement operation to recover the approximated hex GKP, instead of beginning by displacing each input state of the final protocol.

Machine learning optimization algorithms have demonstrated the potential to create high-fidelity GKP states [47] but these methods require in excess of 100 gate operations. The method of photon catalysis we describe here provides an experimentally feasible approach to generate various nonclassical states important for quantum information and quantum computing.

ACKNOWLEDGMENTS

RN would like to thank Lu Zhang for discussions on photon catalysis at QCMC 2018. ME would like to thank Chun-Hung Chang and Jacob Higgins for pointing out an inconsistency in figure scaling. The work is supported by NSF grant No. PHY-1708023.

* me3nq@virginia.edu

- [1] R. P. Feynman, “Simulating Physics With Computers,” *Int. J. Theor. Phys.* **21**, 467 (1982).
- [2] P. W. Shor, “Algorithms for quantum computation: discrete logarithms and factoring,” in *Proceedings, 35th Annual Symposium on Foundations of Computer Science*, S. Goldwasser, ed., pp. 124–134 (IEEE Press, Los Alamitos, CA, Santa Fe, NM, 1994).
- [3] T. D. Ladd, F. Jelezko, R. Laflamme, Y. Nakamura, C. Monroe, and J. L. O’Brien, “Quantum computers,” *Nature (London)* **464**, 45 (2010).
- [4] S. Lloyd and S. L. Braunstein, “Quantum computation over continuous variables,” *Phys. Rev. Lett.* **82**, 1784 (1999).
- [5] S. L. Braunstein and P. van Loock, “Quantum information with continuous variables,” *Rev. Mod. Phys.* **77**, 513 (2005).
- [6] C. Weedbrook, S. Pirandola, R. García-Patrón, N. J. Cerf, T. C. Ralph, J. H. Shapiro, and S. Lloyd, “Gaussian quantum information,” *Rev. Mod. Phys.* **84**, 621 (2012).
- [7] M. Chen, N. C. Menicucci, and O. Pfister, “Experimental realization of multipartite entanglement of 60 modes of a quantum optical frequency comb,” *Phys. Rev. Lett.* **112**, 120505 (2014).
- [8] J.-i. Yoshikawa, S. Yokoyama, T. Kaji, C. Sornphiphatphong, Y. Shiozawa, K. Makino, and A. Furusawa, “Invited Article: Generation of one-million-mode continuous-variable cluster state by unlimited time-domain multiplexing,” *APL Photonics* **1**, 060801 (2016).
- [9] N. C. Menicucci, “Fault-tolerant measurement-based quantum computing with continuous-variable cluster states,” *Phys. Rev. Lett.* **112**, 120504 (2014).
- [10] D. Gottesman, A. Kitaev, and J. Preskill, “Encoding a Qubit in an Oscillator,” *Phys. Rev. A* **64**, 012310 (2001).
- [11] S. Ghose and B. C. Sanders, “Non-Gaussian ancilla states for continuous variable quantum computation via Gaussian maps,” *J. Mod. Opt.* **54**, 855 (2007).
- [12] S. D. Bartlett, B. C. Sanders, S. L. Braunstein, and K. Nemoto, “Efficient classical simulation of continuous variable quantum information processes,” *Phys. Rev. Lett.* **88**, 097904 (2002).
- [13] J. Eisert, S. Scheel, and M. B. Plenio, “Distilling Gaussian States with Gaussian Operations is Impossible,” *Phys. Rev. Lett.* **89**, 137903 (2002).
- [14] J. S. Bell, in *Speakable and unspeakable in quantum mechanics* (Cambridge University Press, 1987), Chap. 21, “EPR correlations and EPW distributions”, pp. 196–200.
- [15] J. Niset, J. Fiurásek, and N. J. Cerf, “No-go theorem for Gaussian quantum error correction,” *Phys. Rev. Lett.* **102**, 120501 (2009).
- [16] A. I. Lvovsky, H. Hansen, T. Aichele, O. Benson, J. Mlynek, and S. Schiller, “Quantum state reconstruction of the single-photon Fock state,” *Phys. Rev. Lett.* **87**, 050402 (2001).
- [17] K. Laiho, K. N. Cassemiro, D. Gross, and C. Silberhorn, “Probing the Negative Wigner Function of a Pulsed Single Photon Point by Point,” *Phys. Rev. Lett.* **105**, 253603 (2010).
- [18] O. Morin, V. D’Auria, C. Fabre, and J. Laurat, “High-fidelity single-photon source based on a Type II optical parametric oscillator,” *Opt. Lett.* **37**, 3738 (2012).
- [19] R. Nehra, A. Win, M. Eaton, N. Sridhar, R. Shahrokhshahi, T. Gerrits, A. Lita, S. W. Nam, and O. Pfister, “Quantum tomography of a single-photon state by photon-number parity measurements,” in *Conference on Lasers and Electro-Optics*, (Optical Society of America, 2019).
- [20] M. Dakna, L. Knöll, and D.-G. Welsch, “Quantum state engineering using conditional measurement on a beam splitter,” *Eur. Phys. J. D* **3**, 295 (1998).
- [21] J. Wenger, R. Tualle-Brouri, and P. Grangier, “Non-Gaussian Statistics from Individual Pulses of Squeezed Light,” *Phys. Rev. Lett.* **92**, 153601 (2004).
- [22] A. Ourjoumtsev, R. Tualle-Brouri, J. Laurat, and P. Grangier, “Generating optical Schrödinger kittens for quantum information processing,” *Science* **312**, 83 (2006).
- [23] V. Averchenko, C. Jacquard, V. Thiel, C. Fabre, and N. Treps, “Multimode theory of single-photon subtraction,” *New J. Phys.* **18**, 083042 (2016).
- [24] A. Zavatta, S. Viciani, and M. Bellini, “Quantum-to-Classical Transition with Single-Photon-Added Coherent States of Light,” *Science* **306**, 660 (2004).
- [25] A. I. Lvovsky and J. Mlynek, “Quantum-Optical Catalysis: Generating Nonclassical States of Light by Means of Linear Optics,” *Phys. Rev. Lett.* **88**, 250401 (2002).
- [26] R. J. Birrittella, M. E. Baz, and C. C. Gerry, “Photon catalysis and quantum state engineering,” *J. Opt. Soc. Am. B* **35**, 1514 (2018).
- [27] D. T. Pegg, L. S. Phillips, and S. M. Barnett, “Optical State Truncation by Projection Synthesis,” *Phys. Rev. Lett.* **81**, 1604 (1998).
- [28] A. E. Lita, A. J. Miller, and S. W. Nam, “Counting near-infrared single-photons with 95% efficiency,” *Opt. Expr.* **16**, 3032 (2008).
- [29] N. Sridhar, R. Shahrokhshahi, A. J. Miller, B. Calkins, T. Gerrits, A. Lita, S. W. Nam, and O. Pfister, “Direct

- measurement of the Wigner function by photon-number-resolving detection,” *J. Opt. Soc. Am. B* **31**, B34 (2014).
- [30] C. M. Caves, “Quantum-Mechanical Radiation-Pressure Fluctuations in an Interferometer,” *Phys. Rev. Lett.* **45**, 75 (1980).
- [31] S. M. Barnett and P. M. Radmore, *Methods in Theoretical Quantum Optics* (Clarendon Press, Oxford, 1997).
- [32] N. C. Menicucci, P. van Loock, M. Gu, C. Weedbrook, T. C. Ralph, and M. A. Nielsen, “Universal quantum computation with continuous-variable cluster states,” *Phys. Rev. Lett.* **97**, 110501 (2006).
- [33] M. Gu, C. Weedbrook, N. C. Menicucci, T. C. Ralph, and P. van Loock, “Quantum computing with continuous-variable clusters,” *Phys. Rev. A* **79**, 062318 (2009).
- [34] M. G. A. Paris, “Displacement operator by beam splitter,” *Phys. Lett. A* **217**, 78 (1996).
- [35] J. R. Johansson, P. D. Nation, and F. Nori, “QuTiP: An open-source Python framework for the dynamics of open quantum systems,” *Comp. Phys. Comm.* **183**, 1760 (2012).
- [36] N. Killoran, J. Izaac, N. Quesada, V. Bergholm, M. Amy, and C. Weedbrook, “Strawberry Fields: A Software Platform for Photonic Quantum Computing,” arXiv:1804.03159 [physics, physics:quant-ph] (2018).
- [37] T. C. Ralph, A. Gilchrist, G. J. Milburn, W. J. Munro, and S. Glancy, “Quantum computation with optical coherent states,” *Phys. Rev. A* **68**, 042319 (2003).
- [38] A. Ourjoumtsev, H. Jeong, R. Tualle-Broui, and P. Grangier, “Generation of optical ‘Schrödinger cats’ from photon number states,” *Nature (London)* **448**, 784 (2007).
- [39] J. S. Neergaard-Nielsen, B. M. Nielsen, C. Hettich, K. Mølmer, and E. S. Polzik, “Generation of a superposition of odd photon number states for quantum information networks,” *Phys. Rev. Lett.* **97**, 083604 (2006).
- [40] H. Takahashi, K. Wakui, S. Suzuki, M. Takeoka, K. Hayasaka, A. Furusawa, and M. Sasaki, “Generation of Large-Amplitude Coherent-State Superposition via Ancilla-Assisted Photon Subtraction,” *Phys. Rev. Lett.* **101**, 233605 (2008).
- [41] T. Gerrits, S. Glancy, T. S. Clement, B. Calkins, A. E. Lita, A. J. Miller, A. L. Migdall, S. W. Nam, R. P. Mirin, and E. Knill, “Generation of optical coherent-state superpositions by number-resolved photon subtraction from the squeezed vacuum,” *Phys. Rev. A* **82**, 031802 (2010).
- [42] A. P. Lund, H. Jeong, T. C. Ralph, and M. S. Kim, “Conditional production of superpositions of coherent states with inefficient photon detection,” *Phys. Rev. A* **70** (2004).
- [43] C. Oh and H. Jeong, “Efficient amplification of superpositions of coherent states using input states with different parities,” *J. Opt. Soc. Am. B* **35**, 2933 (2018).
- [44] D. V. Sychev, A. E. Ulanov, A. A. Pushkina, M. W. Richards, I. A. Fedorov, and A. I. Lvovsky, “Enlargement of optical Schrödinger’s cat states,” *Nat. Photon.* **11**, 379 (2017).
- [45] H. M. Vasconcelos, L. Sanz, and S. Glancy, “All-optical generation of states for “Encoding a qubit in an oscillator,”” *Opt. Lett.* **35**, 3261 (2010).
- [46] K. Noh, V. V. Albert, and L. Jiang, “Quantum capacity bounds of Gaussian thermal loss channels and achievable rates with Gottesman-Kitaev-Preskill codes,” *IEEE Trans. Inform. Theory* pp. 1–1 (2018).
- [47] J. M. Arrazola, T. R. Bromley, J. Izaac, C. R. Myers, K. Brádler, and N. Killoran, “Machine learning method for state preparation and gate synthesis on photonic quantum computers,” arXiv:1807.10781 [quant-ph] (2018).